Photogeneration and charge transport mechanisms in thin films of organic electron acceptor 2,4,7-trinitro-9-fluorenone

2008 J. Phys.: Condens. Matter 20 475205

(http://iopscience.iop.org/0953-8984/20/47/475205)

IOP PUBLISHING JOURNAL OF PHYSICS: CONDENSED MATTER

J. Phys.: Condens. Matter **20** (2008) 475205 (6pp) doi:10.1088/0953-8984/20/47/475205

Photogeneration and charge transport mechanisms in thin films of organic electron acceptor 2,4,7-trinitro-9-fluorenone

I M Kachirski

Peoples' Friendship University of Russia, Moscow, Russia

E-mail: ikachirski@yahoo.com

Received 10 August 2008, in final form 26 September 2008
Published 29 October 2008
Online at stacks.iop.org/JPhysCM/20/475205

Abstract

The photogeneration process in thin films of vacuum-evaporated amorphous 2,4,7-trinitro-9-fluorenone (a-TNF) is investigated by steady-state photoconductivity measurements and by the photoinduced discharge method. It was found that in the intrinsic spectral range of absorption ($\lambda \leqslant 400$ nm) the charge carrier photogeneration mechanism includes several steps. The final step, thermal dissociation of light generated electron–hole pairs, is realized according to the Onsager mechanism. The effect of trapping centers on the conductivity of thin films of a-TNF is investigated by space charge limited current (SCLC), steady-state photoconductivity, and transient photoconductivity methods. It is suggested that the transport of charge carriers in a-TNF is controlled by traps.

1. Introduction

The development of modern photocopying machines, the search for cheap, efficient and reliable solar cells, the search for new conducting materials and molecular storage systems have motivated experimental and theoretical work on organic materials such as molecular crystals, polymers and low-dimensional organic compounds. The organic electron acceptor 2,4,7-trinitro-9-fluorenone is used as a sensitizer of photosensitive polymers, to extend the spectral range of their photosensitivity through the formation of charge-transfer complexes [1]. Thin films of a-TNF can be used as photoconductors or transport layers for electrons in multi-layer photoreceivers [2, 3]. The reported data provide important information on electronic properties of thin films of a-TNF; however, it is still incomplete and insufficient to understand the processes of photogeneration of charge carriers, electron transport in amorphous TNF and the effect of charge trapping centers on the electrical conductivity of a-TNF.

Also, thin films of a-TNF, depending on conditions of sample preparation, can be obtained in amorphous, polycrystalline and crystalline forms [4, 5] and, therefore, this material can be useful to investigate the effects of structure of organic materials on their electrical and photoelectrical properties.

This work is devoted to the investigation of the process of photogeneration of charge carriers in vacuum-evaporated a-TNF thin films and the study of space charge limited current (SCLC) and photoconductivity of this material.

2. Experimental details

a-TNF, used in our experiments, was purified using the method described in [6]. The sandwich-type samples were prepared by the vacuum evaporation technique in a vacuum of 10^{-3} Pa on clean quartz substrates. Electrodes of sandwich samples were made from Ag, Al and SnO_2. We noticed that crystallization centers were developed in a-TNF samples after a few hours of evaporation. Therefore, to avoid the effect of centers of crystallization on electrical and photoelectrical properties of a-TNF films in all our experiments, we used fresh samples.

To investigate the mechanism of photogeneration of charge carriers and to determine the type of charge carriers in a-TNF layers two techniques were used: steady-state photoconductivity measurements in low electric fields ($E_{el} < 10^5$ V cm^{-1}) and the photoinduced discharge method, similar

to that described in [7], in high electric fields ($E_{el} > 10^5$ V cm^{-1}). In the last method, a-TNF was evaporated onto polished aluminum substrates. The sample surface was charged to an initial potential V_0 by placing the sample under a corona discharge. The surface potential was measured by placing the sample under a calibrated transparent electrode connected to an electrometer. The quantum efficiency of production of free charge carriers in a-TNF samples and its dependence on the electric field across the sample were evaluated by measuring the surface potential decrease ΔV under the light exposure. To perform experiments in the quasi-static electric fields the intensity of light pulses was chosen so that the fractional change in the surface potentials was less than 10%.

The steady-state photoconductivity measurements were performed in vacuum at a pressure of 10^{-3} Pa at room temperature. The experimental arrangements and techniques in SCLC and transient photoconductivity experiments were the same as described in [8–10]. The drift mobility of charge carriers in a-TNF samples was measured in transient photoconductivity (time-of-flight) experiments. The packet of free charge carriers in these experiments was generated by pulsed light of 3 ns duration produced by the VSL-337ND pulsed nitrogen laser. The dielectric constant of a-TNF, used in calculation of quantum yield, was obtained from the sample capacitance measured with a multi-frequency LCR meter.

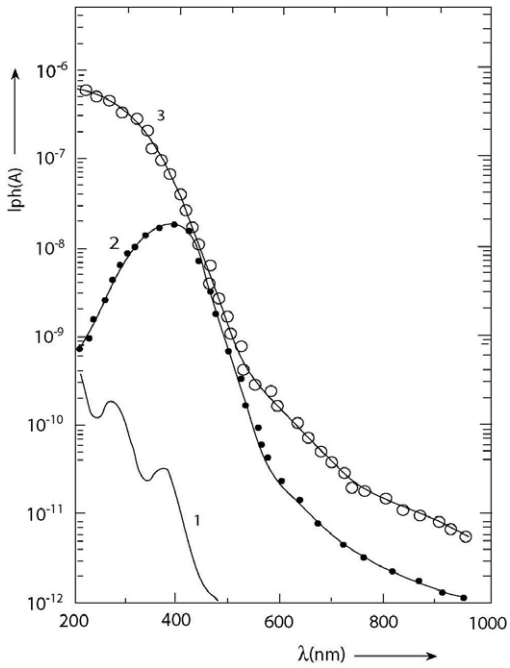

Figure 1. (1) Absorption spectrum of evaporated a-TNF layer and photocurrent spectra of Au/a-TNF/Al sample with (2) positive and (3) negative illuminated Au electrode. $L = 1.2$ μm, $F = 5 \times 10^4$ V cm^{-1}.

3. Results and discussion

In photoconductivity experiments it is found that photocurrent in a-TNF sandwich-type samples reaches the steady state after a few seconds, linearly varies with light intensity and strongly depends on the wavelength of light and the polarity of the electric field across a sample. The typical absorption spectrum and photocurrent spectra of a-TNF thin layers, obtained at different polarities of an illuminated Au electrode, are shown in figure 1. In the long-wavelength range of the spectrum, below the absorption edge ($\lambda > 400$ nm), photocurrent practically does not depend on the polarity of the illuminated electrode, while in the short-wavelength range of the spectrum, where light is strongly absorbed ($\lambda < 400$ nm), photocurrent is considerably higher with the negative potential at the illuminated Au electrode than with the positive potential. This dependence may show that the majority charge carriers in samples of a-TNF are electrons, which is in a good agreement with the results obtained by Gill [12] in amorphous TNF thick layers prepared from melt.

It is found that in the long range of the spectrum photocurrent depends on the material of the illuminated electrodes. Such dependence may indicate that photocurrent in this spectral region of the optical transparency of a-TNF is due to the photoinjection of electrons into the a-TNF films from illuminated electrodes. At shorter wavelengths, the photoinjection is masked by the intrinsic photogeneration mechanism, the contribution of which to the total photocurrent is much higher.

It was found that the photogeneration efficiency in a-TNF strongly depends upon the electric field across the samples because of the recombination process, which is high in low electric fields. To reduce the effect of recombination of charge carriers we investigated the intrinsic photogeneration using the photoinduced discharge method described in [7]. The sample surface was charged to an initial potential V_0 by passing it under a negative corona discharge. To measure the surface potential of the sample it was placed under the transparent calibrated electrode of an electrometer. The sample was then illuminated through the transparent electrode by a high-intensity monochromatic light, which caused a decrease of the surface potential. The quantum yield of photogeneration of charge carriers in a-TNF depends on the electric field, therefore to perform experiments in the quasi-static field the light exposure was chosen so that the fractional change in the surface potential was less than 10%. The change in the surface potential ΔV due to the light pulse was taken as the difference between the initial surface potential V_0 before the exposure and the potential after exposure V, such that $\Delta V = V_0 - V$. The quantum yield of photogeneration of free charge carriers Φ was calculated using the expression

$$\Phi = \frac{\varepsilon\varepsilon_0 \Delta V}{e(1-R)N_\lambda t d},$$

where ε is the dielectric constant ($\varepsilon_{TNF} = 3.3$), $\varepsilon_0 = 8.85 \times 10^{-12}$ F m^{-1}, ΔV is the surface potential change for the exposure time t, e is the electron charge, R is the reflection factor, N_λ is the light intensity in photons cm^{-2} s^{-1}, and d is the sample thickness. The above expression can be applied for calculation of Φ in the case of no recombination of charge carriers in the samples, i.e. if the transit time t_{tr} of charge carriers through the sample is less than the lifetime of the

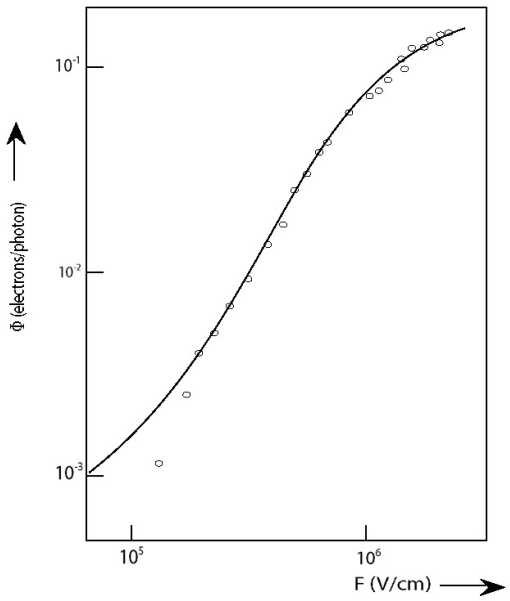

Figure 2. Field dependence of a quantum yield (dots) in TNF amorphous layer. $\lambda = 380$ nm, $L = 1.75$ μm. The solid line is calculated by the Onsager formula with parameters $\Phi_0 = 0.2$ and $r_0 = 2.5 \times 10^{-7}$ cm.

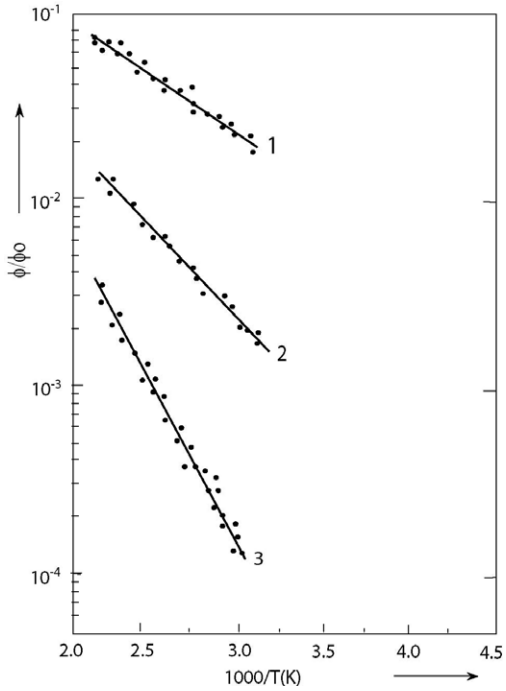

Figure 3. Temperature dependence of the quantum yield of photogeneration in amorphous TNF at different electric fields: (1) $E = 1.0 \times 10^6$ V cm^{-1}, (2) $E = 6.3 \times 10^5$ V cm^{-1}, and (3) $E = 1.0 \times 10^5$ V cm^{-1}, $\lambda = 380$ nm, $L = 1.75$ μm. Dots are experimental results and solid lines are computer simulations on the basis of the Onsager model.

generated carriers. Under these conditions the quantum yield must be independent of sample thickness for the same electric fields. The independence of Φ from d was confirmed in our experiments.

The typical field dependence of Φ in amorphous TNF layers is shown in figure 2, where dots are experimental results calculated from the above formula and the solid line is the computer simulation based on the Onsager diffusion theory [8].

It is assumed that the process of intrinsic photogeneration in organic materials is a multi-step process which proceeds via several intermediate stages: (a) photogeneration of a neutral exciton state, (b) autoionization resulting in creation of a hot quasi-free electron, (c) thermalization of the ejected electron and the formation of a charge-pair (cp) state with quantum yield Φ_0 and with the initial thermalization distance r_0, and (d) thermal dissociation of the cp state into free charge carriers [9]. The last stage is usually described in terms of Onsager diffusion theory, which was originally developed to explain the recombination processes in weak electrolytes and then has been successfully applied to explain photogeneration processes in organic materials [11].

The field dependence of the quantum yield in the a-TNF layer, presented in figure 2, was obtained with 380 nm of monochromatic radiation. As follows from the graph, the field dependence of Φ is characterized by a sharp increase in the field range from 10^5 to 10^6 V cm^{-1} and by saturation in stronger fields. Such dependence may indicate that the process of photogeneration in amorphous TNF is a multi-step process analogous to photogeneration in molecular crystals and conjugated polymers with weak intermolecular or interchain interactions. A good agreement of computation with the experimental results is achieved with the set of parameters $\Phi_0 = 0.2$ and $r_0 = 25$ Å. The large magnitude of λ shows that the charge pairs in a-TNF are generated with high efficiency.

The Onsager diffusion theory implies that the production of free charge carriers is the activated process and the activation energy depends on the electric field in such a way that the higher electric field the less the activation energy. To be sure that the last stage of the intrinsic photogeneration process in a-TNF obeys the Onsager model, the temperature dependence of Φ at different electric fields was investigated. The obtained results are shown in figure 3, where solid lines are computer simulations based on the Onsager theory and dots are experimental results. In calculations we assumed that the thermalization distance r_0 is equal to 25 Å and it is independent of temperature. The results are consistent with predictions of the Onsager theory over the accessible range of electric fields and temperatures.

It was also found that the quantum yield of photogeneration of charge carriers in samples of amorphous TNF strongly depends on the wavelength of the absorbed light. The dependence of Φ on λ is shown in figure 4, where curve 1 is the absorption spectrum of a-TNF and curve 2 is the dependence of Φ on λ. The absorption bands S_1 and S_2 in the absorption spectrum correspond to the transitions between the ground state and the first (S_1) and the second (S_2) excited singlet states of a-TNF, respectively. As follows from the second curve, Φ increases in steps with decreasing λ, which is similar to the absorption spectrum of a-TNF.

From the Onsager diffusion theory it follows that the quantum yield is a function of two quantities, Φ_0 and r_0, and both of these quantities, in principle, can contribute to the dependence of Φ upon λ. To check this prediction of the

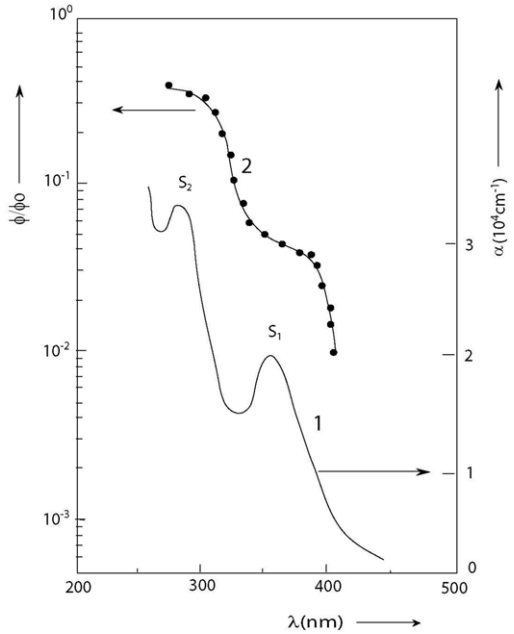

Figure 4. (1) The absorption spectrum of a-TNF. (2) Dependence of the quantum yield on wavelength in a-TNF. $L = 1.75\ \mu$m, $\Phi_0 = 0.2$, and $E = 1.0 \times 10^6$ V cm^{-1}.

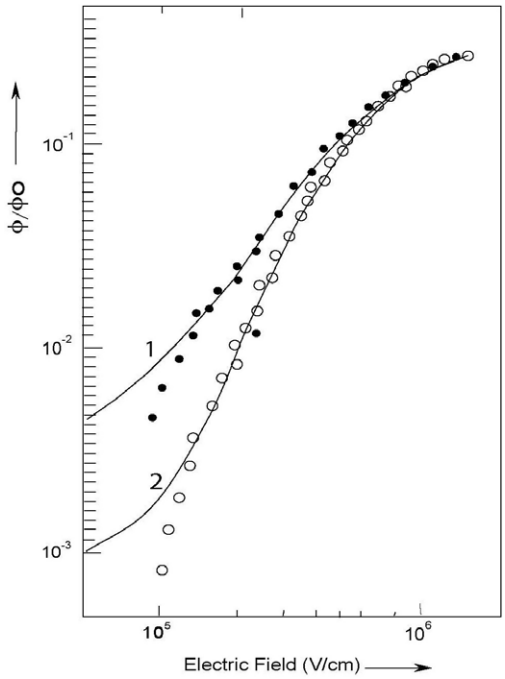

Figure 5. Electric field dependence of the quantum yield in a-TNF at two different wavelengths: (1) $\lambda = 200$ nm, $\Phi_0 = 0.2$, and $r_0 = 27.5$ Å, (2) $\lambda = 385$ nm, $\Phi_0 = 0.2$, and $r_0 = 25$ Å.

Onsager theory the field dependence of Φ at two different wavelengths 280 nm and 385 nm, which correspond to the maxima of two bands, S_1 and S_2, was investigated. The results are illustrated in figure 5, where crosses and dots are experimental results and solid lines are calculations from the Onsager equation with parameters $\Phi_0 = 0.2$ for both wavelengths, $r_0 = 27.5$ Å for $\lambda = 280$ nm, and $r_0 = 25$ Å for $\lambda = 385$ nm. The good agreement of experimental results with computer simulations with chosen parameters Φ_0 and r_0 means that in amorphous TNF the increase in the quantum yield with the decreasing wavelength of absorbed light is due to the dependence of r_0 upon λ only.

To investigate the electronic transport in thin films of amorphous TNF we used SCLC and the transient photoconductivity method. In SCLC experiments it was found that regardless of electrode materials the electric current through the thin films of a-TNF was a non-linear function of the electric field across a sample. The typical current–voltage characteristic (CVC) of a sandwich-type amorphous TNF sample plotted in log–log scale is shown in figure 6 (curve 1). The dots in this graph denote the experimental results and the solid line is the computer simulation of a CVC. As can be seen at the low injecting level, the space charge limited current shows a quadratic dependence on the applied voltage and a superquadratic dependence at higher injecting levels. The dependence of the slope of the CVC is given by $n = \mathrm{d}(\lg J)/\mathrm{d}(\lg V)$ and shown in figure 6 (curve 2). The quadratic dependence of the current density J on applied voltage V in thin films of a-TNF shows the realization of SCLC conditions in our experiments. The observed dependence of the slope of the CVC on the applied voltage cannot be explained on the assumption of the discrete or exponential distribution of charge trapping states in a-TNF samples.

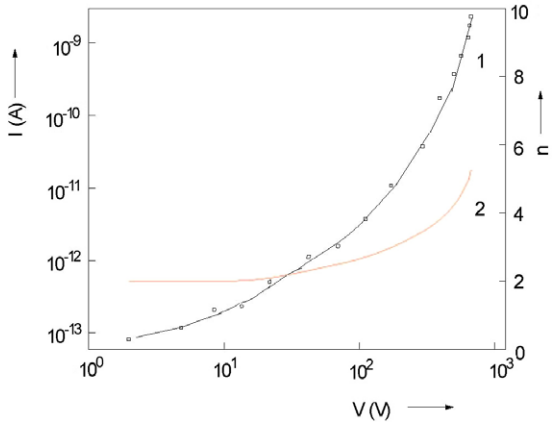

Figure 6. CVC of the Al-a-TNF-Al type sample, sample thickness $d = 8\ \mu$m. The solid line (curve 1) is the calculated curve approximating the experimental points. Curve 2 is $n = f(V)$.

Also, contrary to the predictions of theories based on the discrete and exponential distribution of traps in energy, the observed temperature dependence of SCLC is non-linear. This dependence with voltage as a variable parameter is shown in figure 7, where curve 1 corresponds to the high injection level (300 V) and curve 2 to the low injection level (50 V). Such behavior of SCLC temperature dependence at different injection levels, and also the non-linear dependence of the slope n of the CVC on applied voltage, is evidence for a Gaussian distribution of local trapping states centered in the forbidden energy gap [9]. From the SCLC measurements and computer simulation on the basis of a Gaussian model the effective density of states N_c in the conduction band, the

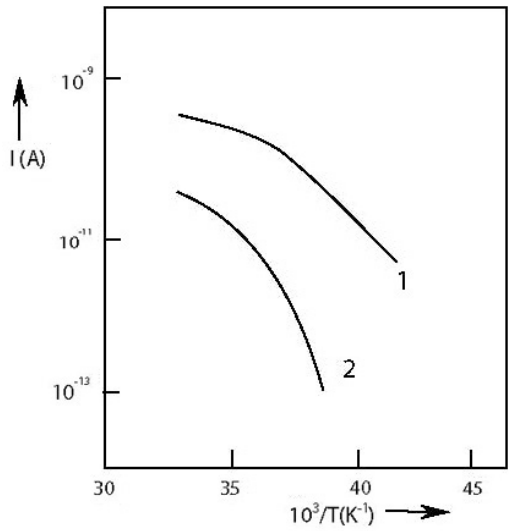

Figure 7. Temperature dependence of SCLC with voltage as a variable parameter. Curve 1—300 V and curve 2—50 V.

Table 1. The charge traps parameters.

Parameter	Method
	SCLC
N_c (cm^{-3})	$(2 \pm 0.2) \times 10^{21}$
N_t (cm^{-3})	$(1 \pm 0.2) \times 10^{17}$
E_t (eV)	0.29 ± 0.04
σ (eV)	0.11 ± 0.02

density of trapping states N_t, the position of the distribution maximum E_t and the distribution parameter σ were evaluated in a-TNF samples. Values of these parameters are given in table 1.

The analysis of the shape of the CVC and the temperature dependence of SCLC indicates that electric fields used in the experiments were insufficient for a complete filling of trapping states; therefore, current through a sample of a-TNF was controlled by charge traps.

In time-of-flight experiments it is found that the majority charge carriers in samples of a-TNF are electrons and the transient photocurrent pulse shows a depressive character. A typical transient photocurrent pulse plotted in a log–log scale is shown in figure 8, where the solid line is the computer simulation on the basis of the theory of depressive transport of charge carriers.

The time corresponding to the change in the slope of the solid line is the transit time t_{tr}. The drift mobility of electrons in a-TNF was calculated with the use of the conventional relation

$$\mu = d/Et_{tr}$$

(E—the electric field across a sample and d—the sample thickness). It was found that the drift mobility of electrons in thin films of a-TNF depends on temperature and on the sweep field. The temperature dependence of μ reveals the activated nature of electron flow. The computed activation energy at an electric field of 3×10^7 V m^{-1} is $E_a = 0.45 \pm 0.03$ eV. The dependence of μ on E in the range of the sweep field

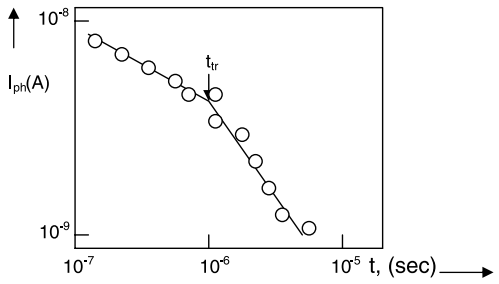

Figure 8. Dependence of the transient photocurrent on time in a-TNV. The solid line is the calculated curve and dots are experimental results.

used in the experiments is similar to that predicted by Poole–Frenkel theory. The zero-field extrapolated activation energy is $E_{a0} = 0.64 \pm 0.04$ eV.

4. Conclusion

Electrons are the majority charge carriers in thin films of a-TNF. This fact is proved by the polarity dependence of the steady-state photocurrent and the transient photocurrent in time-of-flight experiments in sandwich-type samples. The photoconductivity of a-TNF in the short-wavelength range ($\lambda \leqslant 400$ nm) is due to the intrinsic photogeneration. The photogeneration process in a-TNF in the intrinsic region of light absorption is a multi-step process. The final step of photogeneration of charge carriers is realized according to the predictions of the Onsager diffusion theory. The bulk electronic current is controlled by shallow traps with Gaussian distribution centered in the forbidden gap at 0.29 ± 0.04 eV below the conduction level. The fact that the activation energy obtained in SCLC experiments is less than that obtained in time-of-flight experiments may support the suggestion that two processes contribute to E_{a0}: thermally activated transport of electrons and thermal dissociation of electron–hole pairs into free charges. The effect of the sweep electric field on the value of $E_a (E_a < E_{a0})$ is due to the modulation of depth of charge traps by electric field, according to the Poole–Frenkel effect and also due to the dependence of the activation energy of photogeneration of charge carriers on the electric field across a sample, which is in a good agreement with the prediction of the theory of photogeneration of charge carriers in organic semiconductors [11].

References

[1] Gilman P B and Raleigh R G 1971 *US Patent Specification* 3 627 527
[2] Regensburger P J 1973 *Great Britain Patents Specification* 1337 221–227
[3] Karam R E and Swarthoust D J 1975 *US Patent Specification* 3 911 091
[4] Schaffert R 1971 *IBM J. Res. Dev.* **15** 75–80
[5] Turner S R 1980 *Macromolecules* **13** 782–9
[6] Bulyshev Yu S, Kashirskii I M and Sinitskii V V 1984 *Phys. Status Solidi* a **82** 537–44

[7] Emerald R L and Mort J 1974 *J. Appl. Phys.* **45** 3943–9
[8] Bulyshev Yu S, Kashirskii I M and Sinitskii V V 1982 *Phys. Status Solidi* a **70** 139–43
[9] Nespurek S and Silinsh E A 1976 *Phys. Status Solidi* a **34** 747–59
[10] Abdel-Malik T G, Abdeen A M, El-Laban H M and Aly A A 1982 *Phys. Status Solidi* a **72** 99–104
[11] Onsager L 1938 *Phys. Rev.* **54** 554–7
[12] Gill W D 1974 *Proc. Phys. Int. Conf.* vol 2 (London: Garmich-Partenkirchen) pp 901–7